ISSN: 2414-1895 DOI: 10.6919/ICJE.202408_10(8).0008

The Influence of Powder Feeding Rate on the External Flow Field of a Three Channel Coaxial Powder Feeding Nozzle

Shisong Wang*

School of Mechanical Engineering&Automation, Wuhan Textile University, Wuhan, Hubei 430073, China

*1932235520@qq.com

Abstract

This article introduces the numerical simulation of the powder outflow flow field of laser metal deposition (LMD) coaxial powder feeding nozzle software under different powder feeding rates. The simulation results under different powder feeding rates show that as the powder feeding rate increases, the position of the powder convergence point remains unchanged, and the focus is located 14mm below the axis; The powder concentration on the convergence point plane increases, but the powder flow velocity slightly decreases; The powder aggregation area increases, and more powder particles gather on the nozzle axis. The results of this study have certain reference value for optimizing the process parameters of laser metal deposition processing.

Keywords

Additive Manufacturing; Laser Metal Deposition; Powder Flow Behavior; Numerical Simulation; Coaxial Nozzles.

1. Introduction

As an advanced additive manufacturing technology, laser metal deposition (LMD) technology has shown great potential in aerospace, automotive manufacturing, medical devices, and other fields [1-4]. Laser metal deposition technology can be used to manufacture complex aerospace parts[5], repair damaged parts in petrochemical equipment[6], custom-produced mold parts[7], repair and remanufacture of ship parts[8], and customized parts for body structures[9]. LMD technology uses a laser beam to melt and deposit metal powder on the surface of the workpiece, stacking layer by layer to form a three-dimensional part.

Powder feed rate is a key parameter in laser metal deposition technology, which directly affects the velocity field, concentration field and convergence characteristics of the powder external flow field. Proper feed rates ensure a stable deposition process, uniform deposits, and increased construction efficiency, while too high or too low a feed rate can result in degraded sediment quality or wasted material. Numerical simulation is an important means to explore the gas-solid two-phase flow, through which the information of the powder external flow field can be comprehensively analyzed, and the influence of different parameters on the powder external flow field can be explored.

Wang[10] explored the influence of different nozzle outlet shapes on powder aggregation, and the simulation results were basically consistent with the experiments. Fu[11] established a simulation model and used orthogonal experimental methods to explore the optimal process parameters under different conditions of intermediate gas, powder-loaded gas and outer shielding gas. Tan[12] used the finite element method to explore the influence of different particle sizes and elastic recovery coefficients on the powder concentration distribution, and verified them in combination with experiments. Li[13] analyzed the effects of carrier gas flow and powder feed on the powder outflow

ISSN: 2414-1895 DOI: 10.6919/ICJE.202408_10(8).0008

field, and the results showed that the carrier gas flow mainly affected the velocity, while the powder feed mainly affected the concentration. Dong[14] studied the flow law of different process parameters on the powder outflow field, and obtained the velocity field, concentration field, powder flow convergence point position and divergence angle under different parameters, and carried out experimental verification. Karim[15] explored the flow law of the powder flow field, obtained the velocity and concentration distribution of the powder flow field, and analyzed it theoretically. Balu[16] investigated the effects of nozzle structure and carrier gas flow on the focusing height and focusing radius of the powder external flow field, and found the optimal process parameters. Wen[17] used simulation methods to explore the flow and heating process of powder flow, and combined with experiments, the rationality of the simulation results was verified. Zhu[18] explored the distribution of particle concentrations under different cladding layer thicknesses, combined with experimental verification. Wu [19] established a general powder distribution model based on image processing-based powder measurement (IBPM) technology, and the error between the simulated data and the measured data on the axial surface of the powder flow is less than 1%.

In order to explore the influence of powder feeding rate on the powder flow field of coaxial nozzles, a simulation model of the flow field of coaxial powder feeding nozzles was established based on the three-channel coaxial powder feeding model used in the experiment, and compared with the experimental results. The effects of different powder feeding rates on the velocity field, concentration field and convergence of powder outflow field were explored. The particle distribution data on the plane of the convergence point of the powder external flow field is exported by EDEM software.

2. Numerical Model

2.1 Continuous Phase Modeling

In the LMD process, the flow state of the gas is turbulent. According to the flow characteristics of the powder-carrying airflow, the continuous phase is solved based on the Navier-Stakes equation (1) and the standard k-ε turbulence model.

$$\frac{\partial(\varepsilon_f \rho_f)}{\partial t} + \nabla\cdot(\varepsilon_f \rho_f v_f) = 0 \tag{1}$$

The momentum equation is as shown in equation (2):

$$\frac{\partial(\varepsilon_f \rho_f v_f)}{\partial t} + \nabla\cdot(\varepsilon_f \rho_f v_f \mu_f) = -\nabla P + \varepsilon_f \nabla v_f \mu_f + \varepsilon_f \rho_f g - S \tag{2}$$

where ρf is the density of the gas, εf is the porosity, vf is the velocity of the airflow, g is the acceleration due to gravity, μf is the dynamic viscosity of the gas, P is the pressure, and S is the momentum exchange source term.

where the porosity εf is the volume in the grid that is not occupied by particles divided by the volume of the grid elements. The porosity is calculated by counting the number of sample points on the particle surface within the grid, and then dividing this number by the total number of all sample points within the grid, as shown in equation (3):

$$\varepsilon_f = 1 - \sum_{i=1}^{j} \frac{nV_p}{N\Delta V} \tag{3}$$

 Volume 10 Issue 8, 2024
DOI: 10.6919/ICJE.202408_10(8).0008

where n is the number of particle sample points in the grid cell, N is the total number of sample points, VP is the particle volume, j is all particles in the grid cell, and ΔV is the grid cell volume.

The momentum source term S is the volumetric force between the particle and the fluid, as shown in equation (4):

$$S=\frac{1}{\Delta V}\sum_{i=1}^{n}\left\|F_{Di}\right\| \tag{4}$$

where FDi is the resistance to the fluid.

2.2 Discrete Phase Modeling

The discrete phase is based on the Euler-Lagrangian method to establish a motion model, and the equation of motion of the particles is integrated under the Lagrangian method to solve the motion trajectories of the particles.

The particle equation of motion is expressed as Equation (5) and Equation (6):

$$m_p\frac{dv_{pi}}{dt}=m_p g+F_{Bi}+F_{Ci} \tag{5}$$

$$I_{pi}\frac{d\omega_{pi}}{dt}=\sum_{i=1}^{n}T_{pi} \tag{6}$$

where mp is the mass of the particle, FBi is the resistance of the particle, FCi is the collision force of the particle, Ipi is the moment of inertia of the particle, ωpi is the angular velocity of the particle, and Tpi is the resultant moment of the particle.

The empirical formula for the winding resistance FB is shown in equation (7):

$$F_B=\frac{C_d A\rho u_0^2}{2} \tag{7}$$

where Cd is the drag coefficient around the flow, A is the projected area in the direction of the perpendicular incoming velocity of the object, u0 is the incoming velocity of the particles when they are not disturbed, and ρ is the density of the fluid.

2.3 Establishment and Meshing of Computational Domains

The purpose of this study was to investigate the convergence of powders and gases when they interacted, and to investigate the conditions when the carrier gas flow rate was 2 L/min to 10 L/min, and the middle gas flow rate was 10 L/min to 30 L/min. A cylinder with a diameter of 50 mm and a height of 50 mm was chosen as the solution domain, which is more than twice the size of the powder focus. The inlet of the solution domain is set to the velocity inlet and the outlet is set to the pressure outlet.

Meshing with Ansys Meshing software allows you to quickly create fluid meshes of arbitrary complex shapes. During the meshing process, we chose the hexahedral structure because it has a

 Volume 10 Issue 8, 2024
DOI: 10.6919/ICJE.202408_10(8).0008

smaller number of meshes, shorter computation time, and less computational error at the same size. For the outflow field, we used a tetrahedral mesh. The grid size was set to 0.2 mm, and a total of 3297714 grids were generated. As shown in Fig.1, the cylindrical region is set to the air domain, which is large enough relative to the computational domain. Pipe inlets are set to velocity inlet boundary conditions, pipe walls are set to wall surfaces, and outlets are set to pressure outlet boundary conditions.

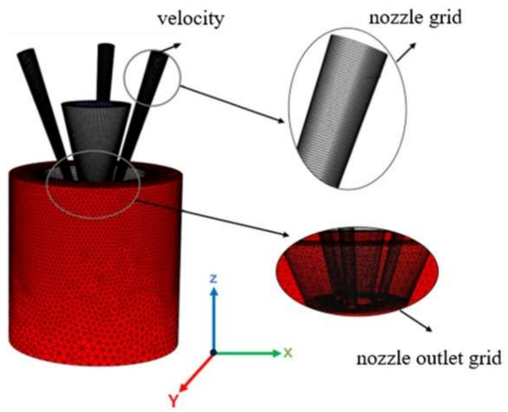

Fig.1 Grid diagram of a three-channel nozzle

3. Numerical Results and Analysis

Powder feed volume in laser metal deposition technology is a crucial parameter that directly affects the concentration and velocity of the powder flow field, which in turn affects the aggregation characteristics of the powder stream, which in turn affects the quality and efficiency of the workpiece forming process. Proper powder feeding can ensure that there is sufficient supply of metal materials in the melting area, so as to form a stable molten pool and improve the molding speed and quality. Excessive or small powder feed can lead to unstable melt pools, affect molding quality, and even cause surface defects and dimensional deviations. Therefore, in practical applications, it is necessary to optimize the process parameters by accurately controlling the amount of powder fed to ensure that the molding quality, accuracy and surface quality of the workpiece meet the design requirements, which is of great significance for improving the process stability and production efficiency of laser metal deposition technology.

The equipment used in this laboratory includes a powder feeder, a robotic arm, a coaxial nozzle, an argon cylinder and a high-speed camera. Table 1 shows the parameter settings of the experiment, and a total of five sets of experimental parameters were set. The relationship between the amount of powder fed and the speed of the powder carousel is shown in Figure 2, and the amount of powder fed is positively correlated with the speed of the powder carousel.

Table 1. Experimental parameter setting table

Number of trials	Carrier gas flow /($L\cdot min^{-1}$)	Shielding gas flow /($L\cdot min^{-1}$)	the speed of the powder disc/(r/min)
1	10	10	4
2	10	10	6
3	10	10	8
4	10	10	10
5	10	10	12

ISSN: 2414-1895 DOI: 10.6919/ICJE.202408_10(8).0008

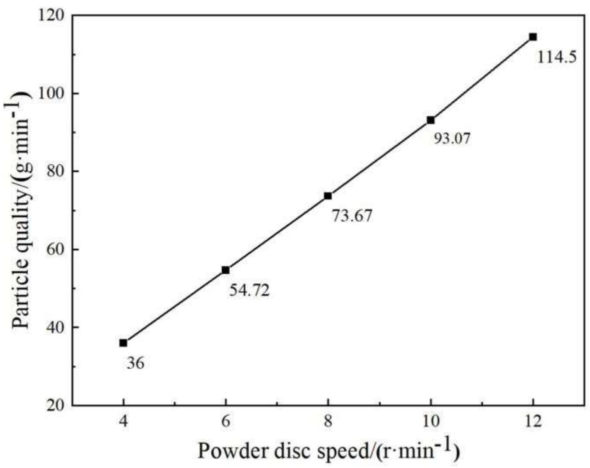

Fig. 2 The amount of powder fed varies with the speed of the powder disc

3.1 Powder Flow Field Observation and Image Processing

In order to intuitively see the pictures of the powder outflow field under different powder feeding amounts, a high-speed camera is used to take pictures of the powder outflow field under different powder feeding amounts. Because the powder flow is too random to visually see the distribution of powder in space, two hundred consecutive images are superimposed with gray values[20]. Due to the large interference of the background of the image after superimposition, the image must be removed by noise first, and then the gray value must be superimposed, as shown in Fig.2. It can be intuitively seen from Fig.3 (a-e) that with the increase of powder feeding, the powder concentration gradually increases, but the convergence height remains unchanged. As the powder flow increases, the powder convergence width gradually increases.

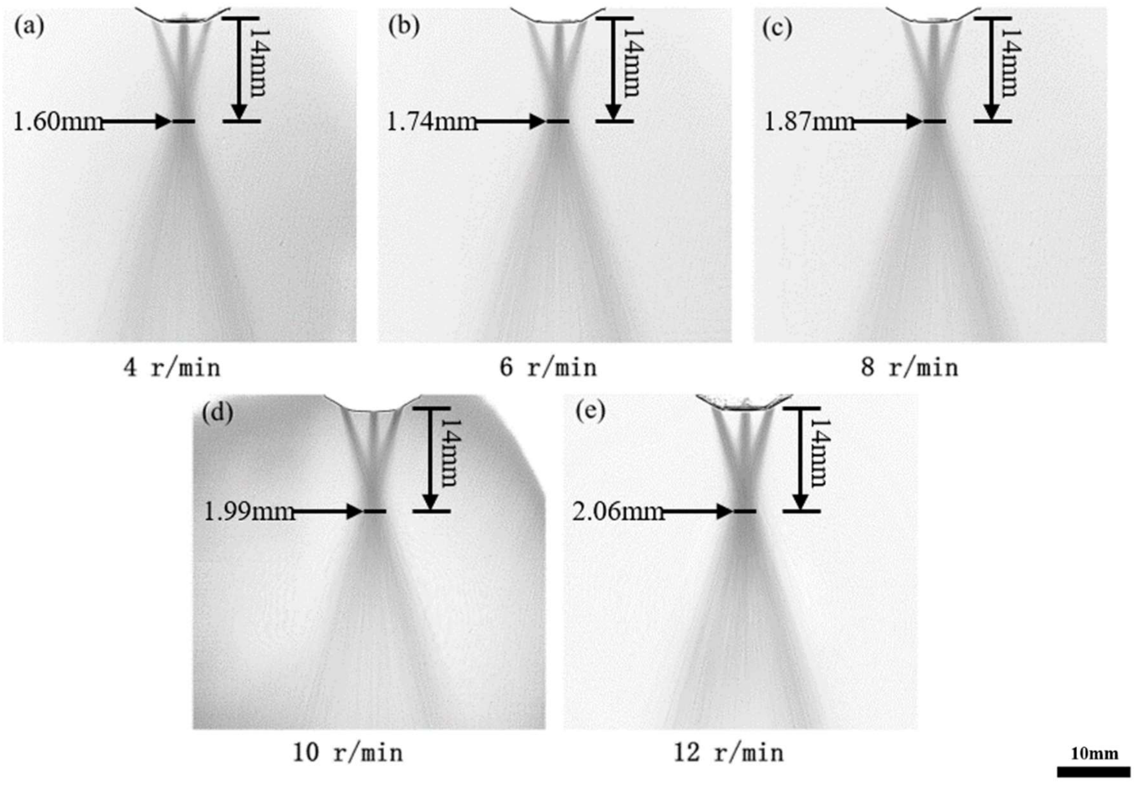

Fig.3 Two hundred consecutive gray value overlays under different powder feeding amounts. (a)4r/min;(b)6r/min;(c)8r/min;(d)10r/min;(e)12r/min

3.2 The Effect of Powder Feed on the Particle Concentration in the Powder External Flow Field

The velocity of the powder particles has an important influence on the spatial distribution of the powder particles in the powder outflow field, so the analysis of the powder velocity is necessary. Fig.4 shows the change in particle velocity at the outlet of the coaxial nozzle at different feed rates. As can be seen in the figure, the velocity of the powder flow at the nozzle outlet decreases from 2.77 m/s at 4 r/min to 2.69 m/s at 12 r/min as the amount of powder fed increases. Excessive powder speed will aggravate the collision of powder, resulting in the divergence of powder flow, thereby reducing the convergence of powder and resulting in low powder utilization, so it is necessary to select the appropriate powder flow.

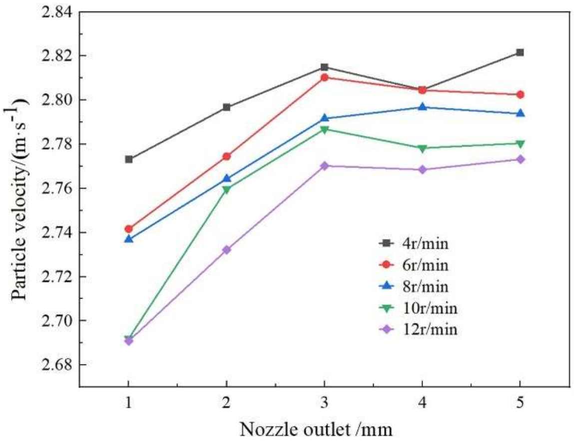

Fig.4 Powder velocity at nozzle outlet at different feed amounts

The point where the powder particle concentration is maximum is usually obtained at the central axis. The distribution of powder on the axis was studied, and the convergence plane of powder particles was found, and then the convergence of powder was studied. Fig.5 shows the distribution of powder concentrations on the central axis at different feed rates, and we can see that the focal position of the convergence does not change with the amount of powder fed. It is evident that there is a "bimodal" distribution of powder concentrations in the curve. The maximum concentration of powder outflow field increased with the increase of powder feeding, from 50.8 kg/m3 at 4 r/min to 220.4 kg/m3 at 12 r/min.

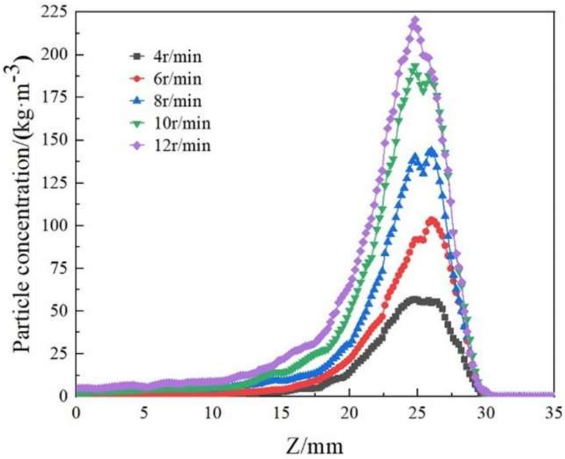

Fig.5 Distribution of particle concentration at the axis under different powder feed rates

ISSN: 2414-1895 DOI: 10.6919/ICJE.202408_10(8).0008

To further understand the spatial distribution of powders, the data from the maximum concentration plane were exported and plotted. Fig. 5 shows the contour of particle concentration at the focal point under different powder feeding amounts, and Fig. 6 (a-e) corresponds to the rotation speed of the powder feeding tray of 4 r/min-12 r/min, respectively. It can be intuitively seen from Fig. 5 that with the increase of powder feed, the powder convergence spots gradually increase, but the increasing trend gradually slows down. In the actual laser metal deposition process, the powder convergence spot should be smaller than the laser spot, and the powder convergence spot is larger than the laser spot, which will make the powder heating insufficient, cause powder waste, and reduce the utilization rate of powder. And the powder that fails to melt will stick to the workpiece, forming internal defects in the workpiece and reducing the mechanical strength of the workpiece. Therefore, in the actual laser metal deposition process, the appropriate powder feeding amount should be selected for the experiment to avoid the impact of the above problems.

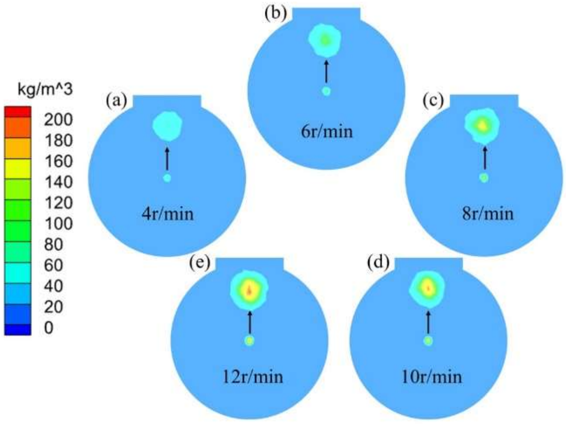

Fig.6 Concentration distribution contour at convergence points under different carrier gas flows.(a)4r/min;(b)6r/min;(c)8r/min;(d)10r/min;(e)12r/min

In order to see the change in the concentration of the powder particles more intuitively, the data of the powder particles in the maximum concentration plane is exported and plotted. Fig.7 shows the powder concentration distribution in the focal plane of the powder external flow field convergence under the condition of 4 r/min to 12 r/min. As can be seen from the figure, with the increase of powder feed, the particle concentration at the convergence focus gradually increases, from 50 kg/m3 at 4 r/min to 200 kg/m3 at 12 r/min, but the increase rate gradually slows down.

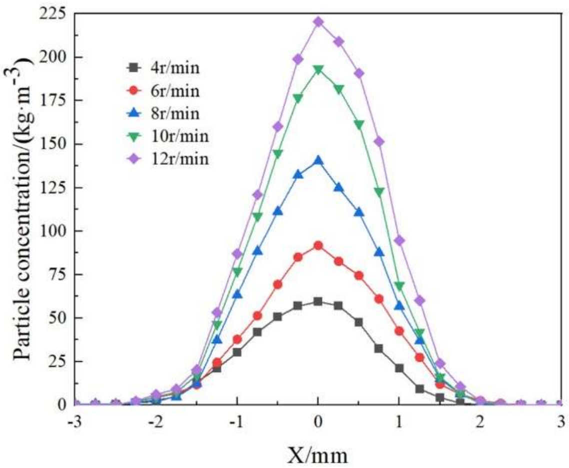

Fig.7 Particle concentration distribution at the convergence plane of the powder external flow field under different powder feeding amounts

ISSN: 2414-1895 DOI: 10.6919/ICJE.202408_10(8).0008

3.3 Effect of Powder Feed on the Convergence of Powder Outflow Field

In order to quantify the powder aggregation under different carrier gas flows, the convergence area under different powder feeding flows was selected as the basis. The pictures of powder spots in the maximum concentration plane under different powder feeding amounts were imported into ImageJ software, and the area curves of powder convergence spots under different powder feeding amounts were obtained, as shown in Figure 8. As can be seen from the figure, the powder aggregation area gradually increased from 20.5 mm2 at 4 r/min to 26.4 mm2 at 12 r/min. With the increase of powder feeding, the area of powder convergence spots gradually increased, but the growth rate gradually slowed down, and the curve gradually converged.

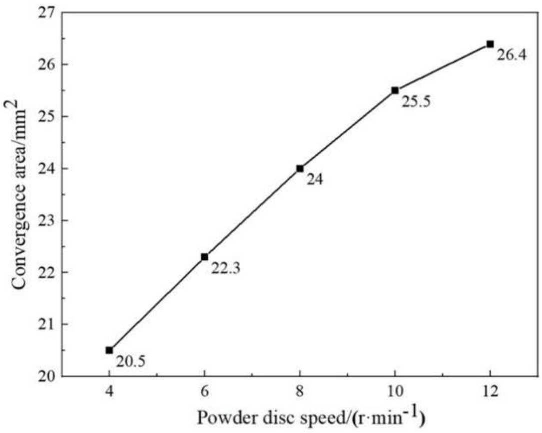

Fig.8 The convergence area at the convergence point at different powder feed rates

In order to clearly see the distribution of the powder at the focal position, the particle position data was imported from the EDEM software into the origin software, and the particle distribution map at the focal position under different powder feeding rates as shown in Fig.9 was plotted. As can be seen in Fig. 8(a), the powder is dispersed at a disc speed of 4 r/min. As the powder flow rate increases, the powder gradually converges towards the center, and the convergence effect becomes better and better, as shown in Fig.9(b-e). As the amount of powder feed increases, the powder collision in the center gradually weakens due to the gradual decrease of powder velocity, so that the powder converges near the axis.

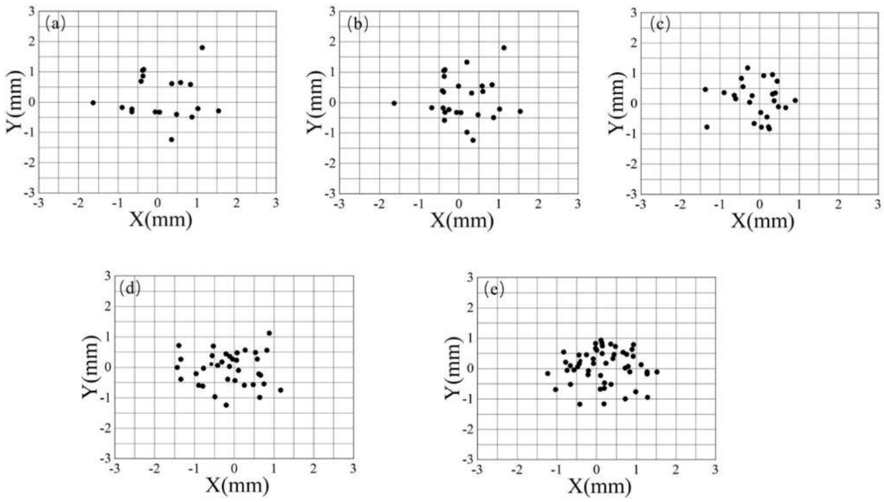

Fig.9 Particle distribution at convergence points at different powder feed rates.(a)4r/min;(b)6r/min;(c)8r/min;(d)10r/min;(e)12r/min

ISSN: 2414-1895 DOI: 10.6919/ICJE.202408_10(8).0008

In summary, when the powder flow rate is small, the powder velocity at the outlet is larger, the powder collision is more intense, and the powder convergence is poor. Therefore, when the powder flow rate is 8 r/min-12 r/min, the powder aggregation is better.

4. Conclusion

In this paper, a three-dimensional simulation model is established based on a three-channel coaxial powder feeding nozzle by combining simulation and experimental verification. According to the theory of gas-solid two-phase flow, the outlet conditions and inlet conditions were reasonably set, and the powder flow characteristics of the coaxial powder feeding process were simulated and verified by experiments by using the discrete element method and the finite volume method. The flow law of powder outflow field under different powder feeding amounts was explored, and the convergence law of powder outflow field affecting powder feeding amount was found. The conclusions are as follows:

(1) The increase in powder feed leads to a decrease in the powder flow rate at the nozzle outlet, from 2.77 m/s at 4 r/min to 2.69 m/s at 12 r/min.

(2) The change of powder feeding volume does not change the height of the focus of powder convergence in the flow field outside the nozzle, and the focus position is 14mm off the axis.

(3) With the increase of powder feeding, the concentration at the maximum concentration of the powder outflow field also increased gradually, from 50.8 kg/m3 at the speed of the powder disc at 4 r/min to 220.4 kg/m3 at the speed of the powder disc at 12 r/min.

(4) The area of the converging spot increased with the increase of powder feed, and the powder convergence area gradually increased from 20.5 mm2 at 4 r/min to 26.4 mm2 at 12 r/min.

References

[1] Wang F.Microstructure Control and Mechanical Behavior of TA19 Alloy Fabricated by Laser Metal Deposition[D].University of Science and Technology of China,2023.

[2] Li F F, Zhao H T,Wang Y L. Study on manufacturing process of TC4 titanium alloy by laser metal deposition technology[J].Nonferrous Metal Materials and Engineering,2023,44(05):68-74.

[3] Yuan G.Numerical simulation and microstructure properties of laser metal deposition TiAl alloy[D].Zhongyuan Institute of Technology,2023.

[4] Liang Z J. Preparation and Research of Self-healing Electrolyte Materials Based on Intrinsic Effect[D].Tianjin University,2022.

[5] Hu M L,Xie C S,Wang A H.Development of Material Consistency of Laser Cladding[J]. Heattreatment of metal,2001(1):1-8.

[6] Ma H B.Study on In-situ Synthesis of Particle Reinforced Composite Coating by Laser Cladding[D]. Dalian University of Technology,2009.

[7] Zhang Q L. Microstructure and Performances of Ultrafine Ceramic Compound Coating Prepared by Laser Cladding[D].Zhejiang University,2013.

[8] Cao H G. Research on H13 Die Steel Semiconductor Laser Haedening and Repairing[D]. Jilin University,2015.

[9] Qiu X W, Li G, Qiu L.The latest Development and Prospects of Laser Cladding Technology[J].Rare metals and cemented carbides.2008,36(3):54-57.

[10] Wang W, Cai L, Yang G, Research on the Coaxial Feeding Nozzle for Laser Cladding. Chinese Journal of Lasers,2012,39(04):73-79.

[11] Fu W, Zhang A F, Li T C, et al. Influences of Three-route Gas Flows on Powder Converging Behavior in Coaxial Powder Feeding Nozzles[J]. China Mechanical Engineering, 2011, 22(02): 220-226.

[12] Tan H,Zhang F Y,Weng R J,Numerical Simulation of Powder Feed of Laser Solid Forming[J].Chinese Journal of Lasers,2011,38(10):46-53.

[13] Li H S.Theoretical and Experimental Study on the Interaction of Laser and Metal Powder Flow in Laser Remanufacturing[D].Tiangong university,2004.

[14] Dong G,Liu J C,Li Y Y.Numerical simulation of gas-powder flow in laser cladding with coaxial powder feeding[J].High power laser and particle beams,2013,25(8):1951-1955.

[15] Karim K, EI-Hachemi A. Numerical Modelling of Gas/Particles Diphasic Jet in Laser Cladding by Coaxial Nozzle. Physics Procedia, 2010, (5): 347-352.

[16] Balu P, Leggett P, Kovacevic R. Parametric study on a coaxial multi-material powder flow in laser-based powder deposition process[J]. Journal of Materials Processing Technology, 2012, 212(7): 1598–1610.

[17] Wen S Y, Shin Y C, Murthy J Y, et al. Modeling of coaxial powder flow for the laser direct deposition process[J]. International Journal of Heat & Mass Transfer, 2009, 52(25– 26): 5867-5877.

[18] Zhu G X, Li D C, Zhan A F, et al. Numerical simulation of metallic powder flow in a coaxial nozzle in laser direct metal deposition[J]. Optics & Laser Technology, 2011, (43): 106-113.

[19] Wu J Z, Zhao P H, Wei H Y, et al. Development of powder distribution model of discontinuous coaxial powder stream in laser direct metal deposition[J]. Power Technology, 2018, 340: 449-458.

[20] Li L Q, Huang Y C, Zou C Y, et al. Numerical Study on Powder Stream Characteristics of Coaxial Laser Metal Deposition Nozzle[J]. Crysrals, 2021, 11(3), 282.